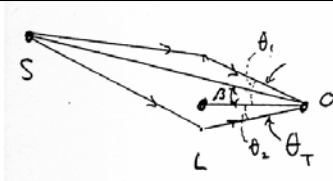


HERE

Effect of Lensing on Flux



Use [CO] notation, but also define

$\theta_T = |\theta_1| + |\theta_2| = \text{total separation between images}$

$$\theta_T = \sqrt{\theta_E^2 + \beta^2}$$

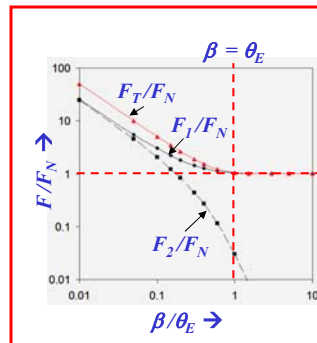
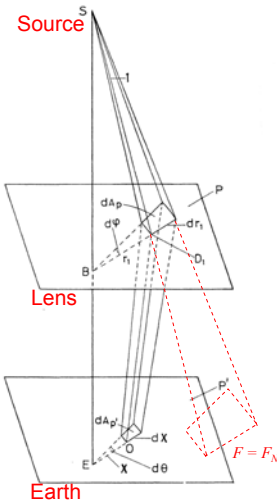
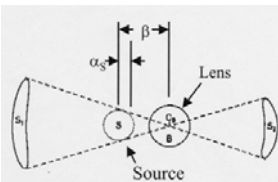
$$F_1 = \frac{1}{4} \left(2 + \frac{\theta_T}{\beta} + \frac{\beta}{\theta_T} \right) F_N$$

$$F_2 = \frac{1}{4} \left(-2 + \frac{\theta_T}{\beta} + \frac{\beta}{\theta_T} \right) F_N$$

$$F_{\text{total}} = F_1 + F_2 = \frac{1}{2} \left[\frac{\theta_T}{\beta} + \frac{\beta}{\theta_T} \right] F_N$$

Lensing of Extended Sources

- Image has same surface brightness as unlensed image, but more area.
- Ring if $\beta < \alpha_S$
- Arcs if $\beta > \alpha_S$
- Max amplification when $\beta = 0 \sim \theta_E / \alpha_S$



Caustics & Catastrophes



Lensing by a Transparent Mass Distribution

$$(ds)^2 = \left(c dt \sqrt{1 - 2GM/rc^2} \right)^2 - \left(\frac{dr}{\sqrt{1 - 2GM/rc^2}} \right)^2 - (r d\theta)^2 - (r \sin \theta d\phi)^2$$

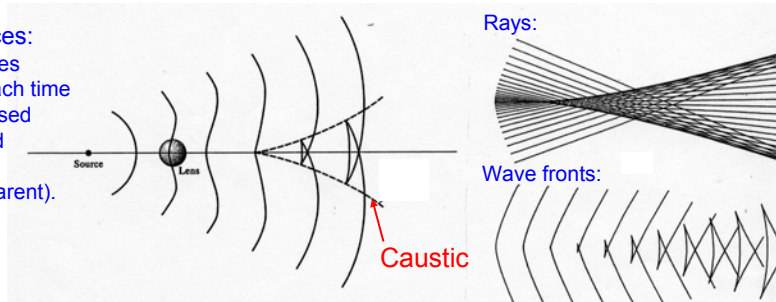
Wavefront retarded by gravitational field:

$$\frac{dr}{dt} = c \left(1 - \frac{2GM}{rc^2} \right)$$

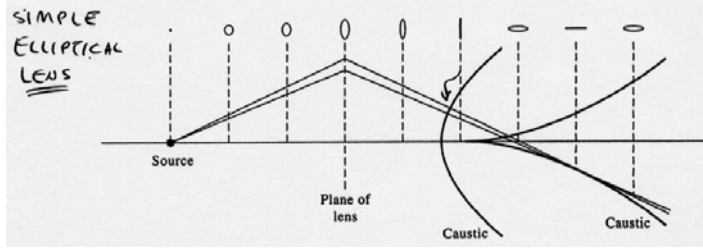
For a transparent mass distribution:

$$(ds)^2 \approx \left(c dt \sqrt{1 + 2\Phi/c^2} \right)^2 - \left(\sqrt{1 - 2\Phi/c^2} \right)^2 (dx^2 + dy^2 + dz^2)$$

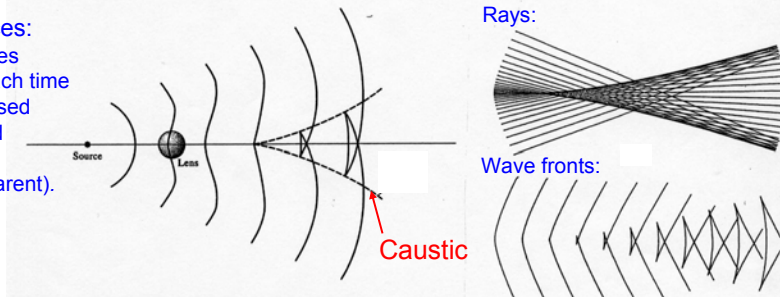
Caustic Surfaces:
 Number of images
 changes by 2 each time
 a caustic is crossed
 → always an odd
 number
 (if lens is transparent).



Lensing by a Transparent Mass Distribution



Caustic Surfaces:
Number of images
changes by 2 each time
a caustic is crossed
→ always an odd
number
(if lens is transparent).



Conjugate Caustic Surfaces

Building blocks are
"elementary catastrophes"

If source object is on one of these surfaces,
observer is on a caustic.

Location of
source
relative to
conjugate
caustics

Resulting
images

Transparent
elliptical lens

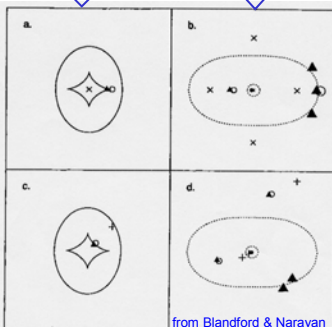
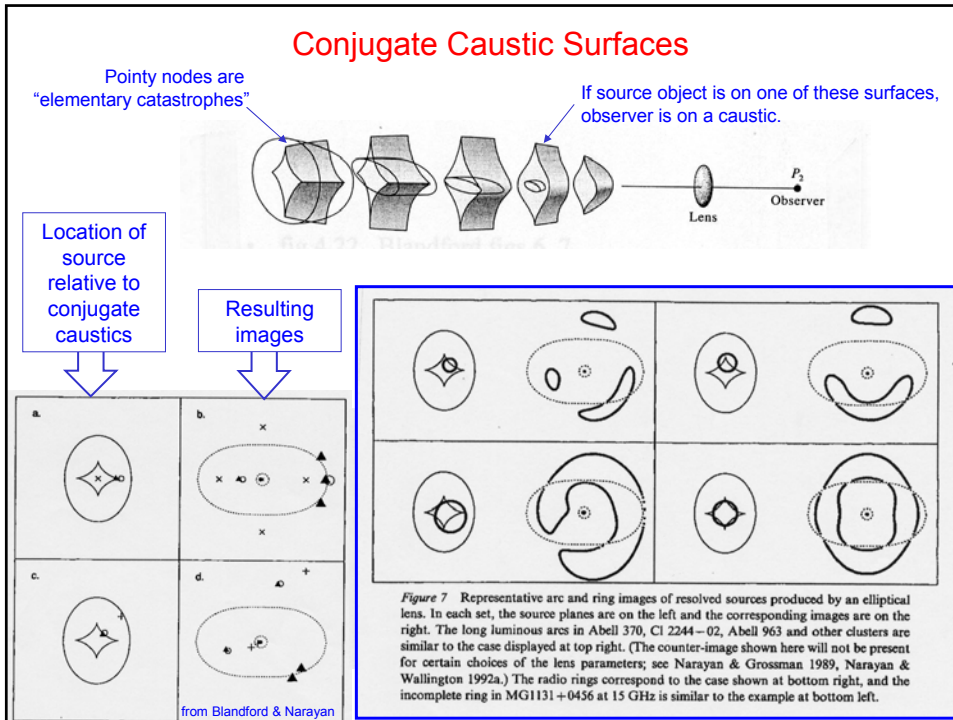
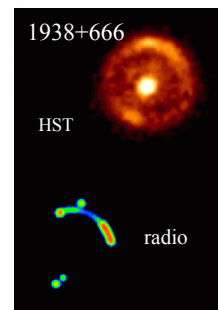
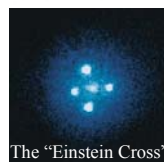


Figure 6 Multiple imaging of point sources at fixed redshift by a generic "elliptical lens." The solid lines in the left panels are *caustics* that separate regions in the source plane corresponding to different image multiplicities (1, 3, and 5 as indicated). The inner caustic, sometimes referred to as the *tangential caustic*, has four cusps connected by fold lines. The outer *radial caustic* is a pure fold. The outer dashed lines in the right panels are tangential critical curves and the inner ones are radial critical curves. The symbols show representative source positions and the corresponding image locations. When the source is close to a caustic, some of the images are strongly magnified, indicated by large symbols in the image panels. One of the multiple images usually occurs near the center of the lens and is strongly demagnified if the core radius of the lens is small. Among the "secure" multiple quasars, Q1413+117 and Q2237+031 correspond to the source position \times and Q0142-100 to \circ in the upper panels. 0414+053 and Q1115+080 correspond to the triangle and Q0957+561 is midway between \circ and $+$ in the lower panels. The weak central image has not been seen in any of the observed cases.



Observations of lensed objects

- Extended background source (e.g. a galaxy)
 - ==> arcs or rings
- Weak lensing: $\theta \gg \theta_E$
 - images slightly extended
 - currently being exploited to look for cluster halos, dark galaxies, etc.
- Strong lensing: $\theta < \theta_E$
 - multiple images formed
 - weak central image usually not seen



Weak (and not-so-weak) Lensing Abell 2218



- Foreground cluster distorts images of numerous background galaxies.
- Use to determine total mass of foreground cluster.
- Shows that 85% of mass is Dark Matter.

Using caustics to search for high-redshift background galaxies

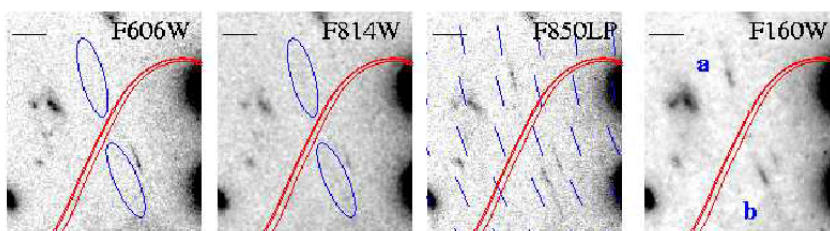
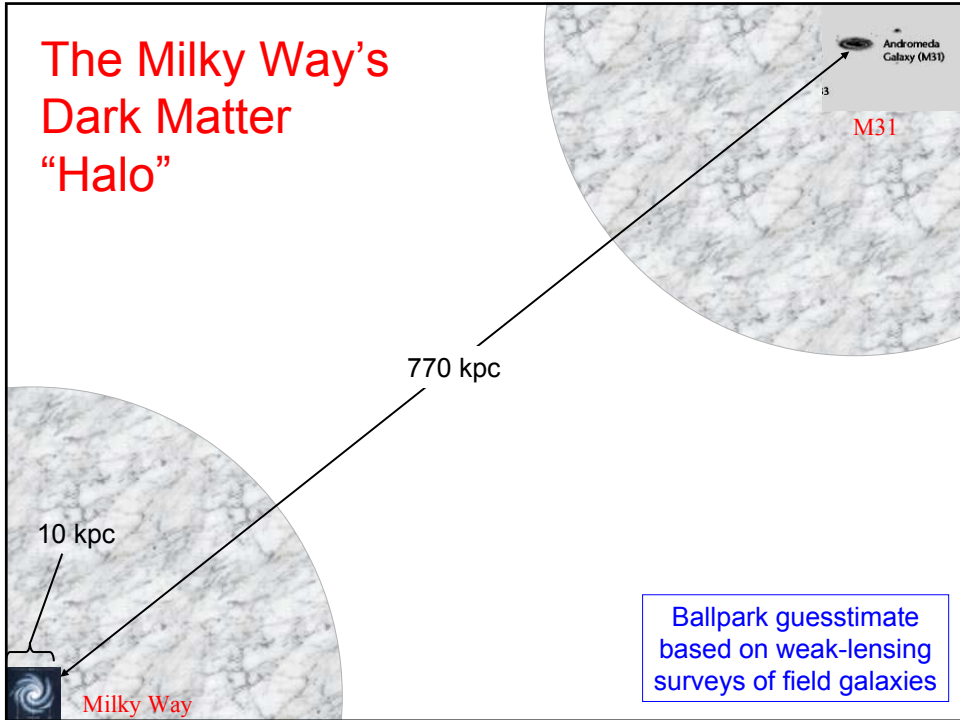
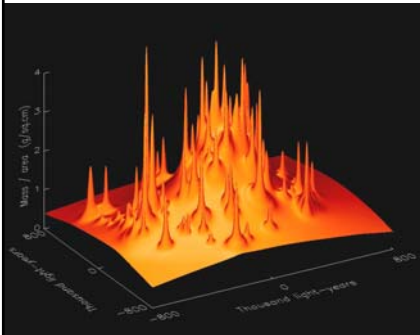


Figure 1: *WFPC2*-F606W, *WFPC2*-F814W, *ACS*-F850LP and *NICMOS*-F160W images of Abell 2218 of the new faint pair in the lensing cluster Abell 2218 ($z=0.175$). The signals redward of the *WFPC2*-F814W observation suggests a marked break occurs in the continuum signal at around 9600\AA . Red lines correspond to the predicted location of the critical lines at $z_s=5, 6.5$ and 7 (from bottom to top, the latter two being almost coincident). The scale bar at the top left of each image represents $2''$. The predicted shear direction (thin blue lines) closely matches the orientation of the lensed images.

The Milky Way's Dark Matter "Halo"

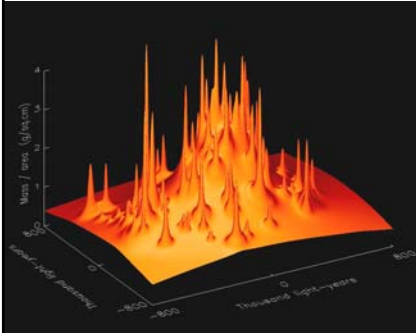


The Remarkable Case of CL0024+1654

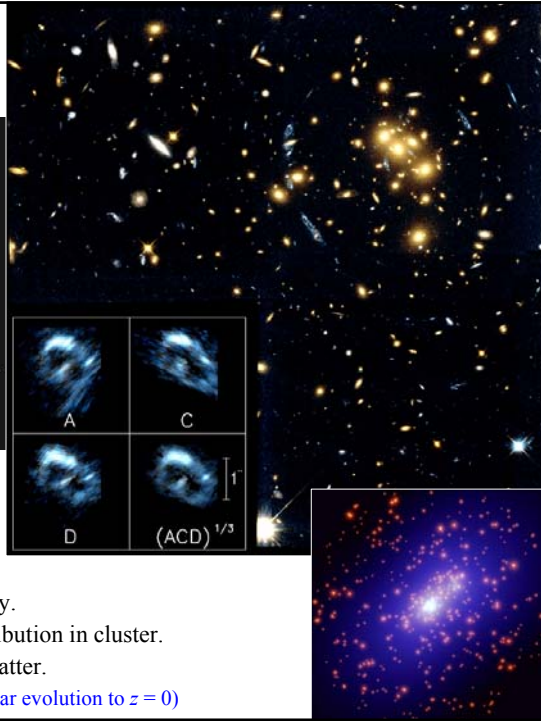


- Single distant blue galaxy
 - $z \sim 1.2 - 1.8$
- Lensed by foreground cluster
 - $z = 0.39$
- 8 different grav. images of blue galaxy.
- Allows detailed analysis of mass distribution in cluster.
- 83% of mass is non-luminous Dark Matter.
- $M/L = 270h$ (390h after allowing for stellar evolution to $z = 0$)

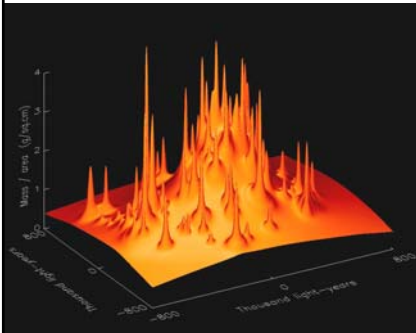
The Remarkable Case of CL0024+1654



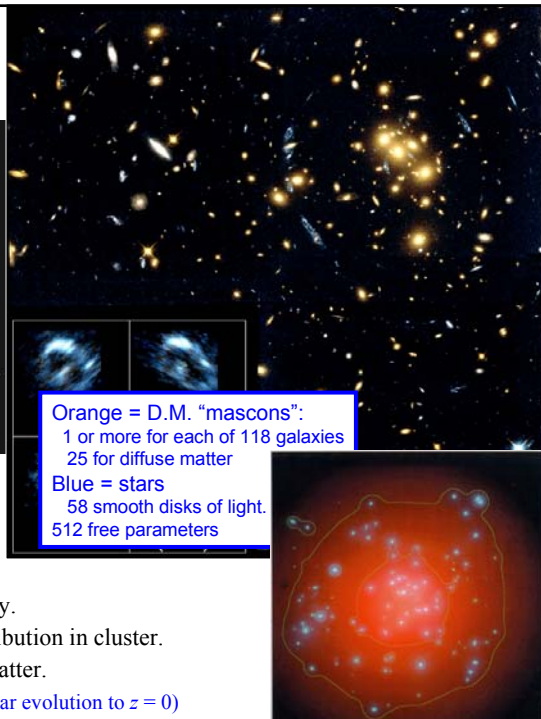
- Single distant blue galaxy
 - $z \sim 1.2 - 1.8$
- Lensed by foreground cluster
 - $z = 0.39$
- 8 different grav. images of blue galaxy.
- Allows detailed analysis of mass distribution in cluster.
- 83% of mass is non-luminous Dark Matter.
- $M/L = 270h$ ($390h$ after allowing for stellar evolution to $z = 0$)



The Remarkable Case of CL0024+1654



- Single distant blue galaxy
 - $z \sim 1.2 - 1.8$
- Lensed by foreground cluster
 - $z = 0.39$
- 8 different grav. images of blue galaxy.
- Allows detailed analysis of mass distribution in cluster.
- 83% of mass is non-luminous Dark Matter.
- $M/L = 270h$ ($390h$ after allowing for stellar evolution to $z = 0$)



Orange = D.M. "mascons":
 1 or more for each of 118 galaxies
 25 for diffuse matter
 Blue = stars
 58 smooth disks of light.
 512 free parameters